



On the prospective detection of polyoxymethylene in comet 67P/Churyumov–Gerasimenko with the COSIMA instrument onboard Rosetta

Léna Le Roy^{a,b}, Giacomo Briani^{b,1}, Christelle Briois^a, Hervé Cottin^{b,*}, Nicolas Fray^b, Laurent Thirkell^a, Gilles Poulet^a, Martin Hilchenbach^c

^a Laboratoire de Physique et Chimie de l'Environnement et de l'Espace (LPC2E), UMR 6115 CNRS – Université d'Orléans, 3A Avenue de la Recherche Scientifique, 45071 Orléans Cedex 2, France

^b Laboratoire Interuniversitaire des Systèmes Atmosphériques, LISA, UMR CNRS 7583, Université Paris Est Créteil et Université Paris Diderot, Institut Pierre Simon Laplace, 61 Avenue du Général De Gaulle, 94010 Créteil Cedex, France

^c Max Planck Institute for Solar System Research (MPS), Max-Planck-Str. 2, 37191 Katlenburg-Lindau, Germany

ARTICLE INFO

Article history:

Received 4 August 2011
Received in revised form
23 January 2012
Accepted 25 January 2012
Available online 7 February 2012

Keywords:

Polyoxymethylene
Cometary grains
COSIMA
Rosetta
TOF SIMS

ABSTRACT

The presence of polyoxymethylene (POM) in cometary grains has been debated years ago. Although never proven, its presence can not be excluded. Rosetta, the ESA mission to comet 67P/Churyumov–Gerasimenko, may answer this question. On board the spacecraft, COSIMA (COMetary Secondary Ion Mass Analyzer) will analyze the grains ejected from the nucleus using a Time Of Flight Secondary Ion Mass Spectrometer (TOF-SIMS). In this paper we report the extent to which COSIMA will be able to detect POM if this compound is present on cometary grains. We have analyzed two kinds of POM polymers with a laboratory model of COSIMA. Positive mass spectra display alternating sequence of peaks with a separation of 30.011 Da between 1 and 600 Da related to formaldehyde and its oligomers but also to the fragmentation of these oligomers. The separation of 30.011 Da of numbers peaks, corresponding to the fragmentation into H₂CO is characteristic of POM and we show that it could be highlight by mathematical treatment. POM lifetime on COSIMA targets have also been studied as POM is thermally instable. It can be concluded that the cometary grains analysis have to be planned not too long after their collection in order to maximize the chances to detect POM. This work was supported by the Centre National d'Etudes Spatiales (CNES).

© 2012 Elsevier Ltd. All rights reserved.

1. Introduction

Comets are considered as the most pristine remainders of the Solar System formation, and they could have delivered water and organic molecules on the primitive Earth (Delsemme, 1999; Oro et al., 2006). Thus, the study of comets is interesting for planetology and astrobiology: their analysis can provide insights into physical and chemical conditions in the early Solar nebula (Irvine and Lunine, 2004) and on the nature of organic molecules delivered on the early Earth (Anders, 1989; Chyba and Sagan, 1992; Oro, 1961). The knowledge of the chemical composition of comets is therefore important for our understanding of the Solar System formation and the emergence of life on Earth.

The volatile phase of the cometary environment has been extensively studied by remote sensing instruments. More than

twenty five gaseous species have already been identified in their coma (Bockelée-Morvan et al., 2004; Feldman et al., 2004), from which models regarding the composition of nuclei ices can be derived. Numerous minerals have been detected in cometary grains thanks to remote infrared spectroscopy (Crovisier et al., 1997) and to the analysis of the cometary grains returned on Earth by the Stardust mission (Zolensky et al., 2006). The presence of refractory organic compounds on cometary grains has been revealed by the Giotto and Vega mission (Kissel et al., 1986a, b), and confirmed by the Stardust mission (Sandford et al., 2006). But their exact nature is still uncertain due to the difficulty to analyze the organic phase of cometary grains or the nucleus directly.

Several in-situ missions have taken measurements related to the composition of solid organic compounds in cometary grains. To date, four missions (Vega 1 & 2, Giotto and Stardust) have provided results: in 1986 the time-of-flight mass spectrometers PUMA 1 & 2 and PIA, respectively onboard the Soviet missions Vega 1 & 2 and onboard the European Space Agency (ESA) mission Giotto, have made the first in situ analysis of grains ejected from the nucleus of the comet 1P/Halley (Kissel et al., 1986a, b). The mass spectra collected by PUMA highlighted the presence of

* Corresponding author. Tel.: +33 1 45 17 15 63; fax: +33 1 45 17 15 64.

E-mail address: Herve.Cottin@lisa.u-pec.fr (H. Cottin).

¹ Present address: Centre de Spectrométrie Nucléaire et de Spectrométrie de Masse (CSNSM), UMR 8609, Université Paris Sud/CNRS, Bat. 104, F-91405 Orsay Campus, France.

different kind of grains: rocky grains, CHON grains (i.e., grains constituted of C, H, O and N atoms) and grains made of rocky elements and organics, which could be intermixed on the sub-micron scale (Jessberger et al., 1988). The organic part in the grains is important in Halley's dust. It represents about 50% in mass, the remaining 50% being due to the minerals (Fomenkova et al., 1994). It also appeared that these organic compounds are more complex than expected (i.e., mass spectra displayed features for mass greater than 100 Da) (Kissel et al., 1986a). However, only assumptions about the nature of those compounds can be made due to the very short observation duration of the comet (1.5 h), the break-up of the parent compounds on high-velocity impacts on the metal targets and the limited mass resolution of instruments (Krueger and Kissel, 1987). The mass resolution is defined as $m/\Delta m$; here Δm is the Full Width at Half Maximum (FWHM) of a peak centered at the mass m . It was about 100 and 200 at $m/z=100$ for PUMA 1 & 2 and PIA, respectively (Lawler et al., 1989).

In 2006, the analysis of the samples returned by the NASA's Stardust spacecraft highlighted the presence of crystalline silicates as well as complex organic matter (aromatic, aliphatic and N-containing functional groups) in grains of comet 81P/Wild 2 (Sandford et al., 2006; Sandford et al., 2010; Zolensky et al., 2006). Since these preliminary results, more analyses have been performed and revealed the presence of glycine, the simplest amino acid (Elsila et al., 2009). The Stardust spacecraft also made in situ measurements, with CIDA (Cometary Interstellar Dust Analyser), an onboard particle impact time-of-flight mass spectrometer. Its measurements highlighted that nitrogen-containing species are an important part of the cometary dust particles (Kissel et al., 2004).

The forthcoming space mission related to cometary studies is the Rosetta mission. This ESA mission, launched in March 2004, will perform the most exhaustive study ever done of a comet after a ten years journey (Glassmeier et al., 2007). Its target is the Jupiter family comet 67P/Churyumov–Gerasimenko (67P/CG). The probe consists of two parts: an orbiter, to study the comet for at least one year and a half during its approach to the Sun, and a lander, to perform analyses directly on the nucleus during at least five days.

Onboard the probe, several instruments will measure the chemical composition of refractory organic material:

- COSIMA (COmetary Secondary Ion Mass Analyzer) is a mass spectrometer designed to collect and analyze the cometary grains (Kissel et al., 2007). COSIMA is a TOF-SIMS (Time of Flight Secondary Ion Mass Spectrometry), which analyzes the first few atomic layers of a solid sample and then enables the measure of the chemical composition of grains and notably of refractory organic matter. Its mass resolution ($m/\Delta m$) better than 1500 at $m/z=100$, is at least 10 times better than the one of the mass spectrometers on board the Stardust, Giotto and Vega missions. The grains will be collected on metallic targets at about 100 m/s (Kissel et al., 2007). Thus the cometary matter will not be vaporized and turned into a hot plasma as for previous missions, for which the impact velocity of grains was 6, 69 and 78 km/s for Stardust, Giotto and Vega 1 & 2, respectively (Brownlee et al., 2006; Langevin et al., 1987).
- VIRTIS (Visible InfraRed thermal Imaging spectrometer) is a spectral imager, onboard the orbiter, which covers the 0.25 to 5 μm wavelength range. It will detect and characterize spectral bands of minerals and molecules arising from surface and from grains dispersed in the coma (Coradini et al., 2007).
- COSAC (COmetary Sampling and Composition experiment) is a gas chromatograph coupled with a time of flight mass spectrometer ($m/\Delta m=350$ at the peak FWHM at $m/z=70$) on board the lander PHILAE. It will analyze samples from the surface

and subsurface of 67P/CG nucleus and allow the characterization and quantification of organic compounds including large and chiral molecules by heating them up to 327 K (Goesmann et al., 2007).

- MODULUS-Ptolemy (Methods of Determining and Understanding Light elements from Unequivocal Stable isotope compositions) is an instrument onboard the lander centered around an ion trap mass spectrometer ($m/\Delta m=66$ at the peak FWHM at $m/z=44$, this mass resolution has been calculated from the mass spectrum of Ptolemy qualification model; it could be improved, if required, but the intensity of the signal will decrease). Its aim is to determine the nature and isotopic compositions of gases and refractory compounds at the surface and sub-surface of the nucleus. These measurements will be done directly for gaseous species and by converting solid compounds into gases using various thermal and chemical techniques. Gases can be analyzed directly by the mass spectrometer, or via gas chromatography columns or through chemical processing modules before the mass spectrometer analysis (Wright et al., 2007).

In this paper, we focus on the detection of the formaldehyde polymer polyoxymethylene (POM, $(\text{H}_2\text{CO})_n$) with COSIMA. The presence of POM on grains of comet 1P/Halley has been claimed in 1987 by Huebner (1987). Indeed mass spectra acquired by the PICCA instrument displayed a regular pattern of peaks with alternations of 14 and 16 Da (Da) that Huebner (1987) linked this to the sequence of $-\text{CH}_2-$ ($m=14$ Da) and $-\text{O}-$ ($m=16$ Da) fragments, and then to POM. However Mitchell et al. (1992) have shown that this pattern can be relevant of any kind of complex mixture made of C, H, O, N atoms. Thus the presence of POM has never been confirmed, or excluded. Nevertheless some clues point towards its presence:

- POM or POM-like polymers are synthesized during thermal processing or UV irradiation of cometary ice analogs (Bernstein et al., 1995; Schutte et al., 1993a, b; Vinogradoff et al., 2011).
- Its presence in cometary grains and its thermal decomposition into gaseous formaldehyde is an efficient way to explain the observation of the distributed source (i.e., production of gaseous product by photo and/or thermal degradation of refractory carbonaceous matter in coma) of gaseous formaldehyde in cometary atmospheres. Indeed only a few percent in mass of POM in grains could explain this distributed source (Cottin et al., 2004; Cottin and Fray, 2008; Fray et al., 2006).

COSIMA is surely the most appropriate instrument to detect directly POM in comet 67P/CG. Indeed the major infrared spectral features of POM are close to 10 μm , whereas VIRTIS will probe the coma only up to 5 μm . COSAC and MODULUS-Ptolemy will involve indirect detection of POM because solid samples have to be heated to temperatures at which POM decomposes into formaldehyde. So, only a formaldehyde excess can be measured with these two instruments.

The goal of this paper is to study the extent to which COSIMA could detect POM if this organic compound is present in the grains of comet 67P/CG.

The polyoxymethylene has specific chemical properties, which could enhance or decrease the possibility of its detection. POM is a generic name for formaldehyde polymers. Usually, its terminal group is an hydroxyl group (OH) which gives the general formula: $\text{HO}-(\text{CH}_2\text{O})_n-\text{H}$ with n the number of monomers (Walker, 1964). Two other common terminal functions are: the methylether function (CH_3O) and the acetate function (CH_3CO), which lead, respectively to $\text{CH}_3\text{O}-(\text{CH}_2\text{O})_n-\text{CH}_3$ and $\text{CH}_3\text{CO}-(\text{CH}_2\text{O})_n-\text{COCH}_3$ (Bevington and May, 1964; Pchelintsev et al., 1988).

POM has different designations as a function of chain length (number of monomers) and of terminal group. These differences confer to POM specific chemical properties such as difference on its thermal stability. POM thermal decomposition proceeds by a zipper mechanism initiated at chain end, up to about 530 K, producing gaseous formaldehyde as the only reaction product (Zimmermann and Behnisch, 1982). For instance, POM with OH as terminal group is thermally less stable than POM with an acetate function as a terminal group.

Obviously, if there is some POM in the grains of 67P/CG, its exact nature is unknown. COSIMA would give us some hints. Due to POM instability, the temperatures that cometary grains can reach in COSIMA have to be considered in order to propose optimal tasks to detect POM.

Fig. 1 represents a schematic view of COSIMA. COSIMA contains several units: (i) a storage area for 72 targets, (ii) a target manipulator unit (TMU) to handle the transport of targets between individual stations, (iii) a dust collection position where cometary grains could be collected onto targets, (iv) an optical microscope system (COSISCOPE) to image each target and locate precisely the grains, (v) a chemistry station, in which a target can be heated up to 403 K and (vi) the TOF-SIMS.

Depending on its location, targets are submitted to different temperatures. In the storage area, the temperature should be below 303 K (Kissel et al., 2007). When they are brought to the dust collection position, temperature can drop to about 253 K (the coldest one that targets can reach). After the collection, they are moved to the microscope position to localize the grains and then in front of the TOF-SIMS. Temperature at microscope and analysis position should be below 303 K. The target could also be brought inside a chemistry station where the samples can be heated up to 403 K.

Rosetta trajectories and timelines after lander delivery in 2014 are currently being discussed and planned by ESA. Therefore all COSIMA operations are not yet planned, such as the time between the collection of a grain and its analysis. Another critical parameter has to be taken into account: a delay of about a week between new programming operation from Earth and its application in space. As POM is thermally unstable, long storage duration without any analysis could compromise its detection if POM disappears from the grains before the analysis.

In this paper, TOF-SIMS analysis (with a ground analog instrument of COSIMA) and decomposition kinetics studies of different kind of POMs are reported. Our goals are to measure reference spectra to enable POM identification with COSIMA, and to estimate POM lifetime to define a COSIMA operational strategy allowing a clear detection of POM if present in cometary grains.

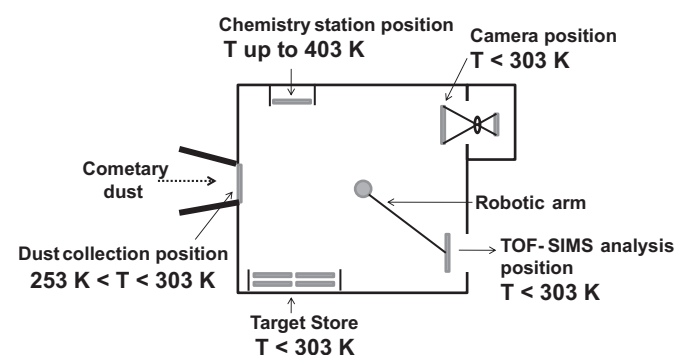


Fig. 1. Schematic view of COSIMA based on Kissel et al. (2007). The temperatures that cometary dust could encounter in COSIMA are reported.

2. Experimental

2.1. Analytical techniques

2.1.1. FTIR spectroscopy

Fourier Transform InfraRed (FTIR) spectroscopy has been operated to compare the two kinds of POM used in this study (commercial and synthesized), to check the repeatability of laboratory analog syntheses and to follow the evolution of the POM as a function of time during kinetic studies.

The spectrum of the commercial product (“POM Com”) has been analyzed in KBr pellets at a resolution of 4 cm^{-1} , whereas the spectra of the laboratory analogs (“POM Lab”) have been measured inside a high vacuum chamber on a CsI or MgF_2 window, where they are synthesized, at a resolution of 0.5 cm^{-1} .

2.1.2. TOF-SIMS

The TOF-SIMS used in this study is a laboratory model of COSIMA developed and located in LPC2E (Orléans), having similar instrumental characteristics such as the mass resolution ($m/\Delta m = 2000$ at the peak FWHM at $m/z = 100$) and having the same Primary Ion Beam System (PIBS).

The instrument consists of a pulsed primary indium ion beam ($^{115}\text{In}^+$) which is focused onto the sample. This bombardment induces the release of atoms, neutral molecules, positive and negative secondary ions from the first three monolayers of the sample. The secondary ions are then focused on the detector which is a micro-channel plate.

The output cumulated signal gives the number of detected secondary ions versus time. This time corresponds to the flight duration that ions take to go from the target to the detector. The conversion of time into mass is calculated using the assumption that some peaks measured in the spectrum (e.g., H, C, Na, In or Au) are known.

As both positive and negative secondary ions are released from the sample, spectra are measured in both modes (positive & negative). The measurement of the secondary ions is made between 1 and 600 Da (Da) but can be extended to higher mass ranges (up to 19,440,000 Da) if needed. The mass spectra sampling is smaller than the width of the observed peaks (For instance Hydrogen peak has a FWHM of 0.039 Da and the sampling of this peak is 0.009 Da). During all the experiments, the vacuum pressure inside the analysis chamber is about 1×10^{-9} mbar.

2.1.3. Sample preparation and control spectra analysis

For the analysis, gold targets (purity 99.95%, Goodfellows) were cleaned in ultrasonic bath of *n*-hexane and then acetone to remove any kind of contamination. For each sample, two sets of TOF-SIMS analysis were performed. A first set of spectra is acquired before sample deposition to reference the nature and the level of the surface contamination. After this step, POM samples are deposited on the cleaned target and gently crushed with an agate pestle to obtain thin deposit. The second series of spectra is then measured.

2.2. Samples

If any, the exact nature of POM in comets is unknown. It must be rather fragile and easily decomposed into formaldehyde to account for the observed distributed formaldehyde source. Therefore, we have selected two kinds of POM for our analyses. The first one is a paraformaldehyde ($(\text{HO}-(\text{CH}_2\text{O})_n-\text{H})$ with n ranging from 6 to 100) (Prolabo, purity > 99.5%). Later in this paper, it will be referred as “POM Com”. The second one (“POM Lab”) is a laboratory analog synthesized under conditions relevant to

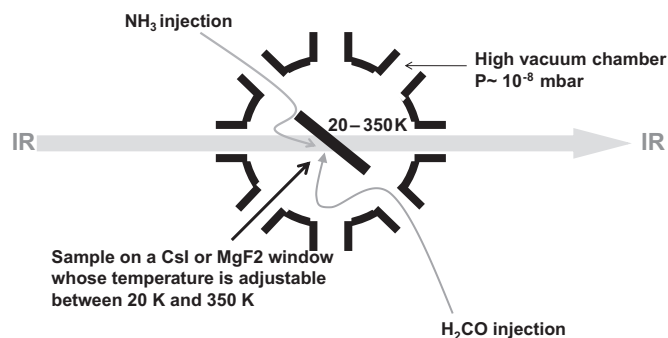


Fig. 2. Schematic view of OREGOC setup. The sample is deposited on a Csl or MgF₂ window whose temperature is adjustable between 20 and 350 K.

chemistry of interstellar and cometary ices (see details of synthesis in Section 2.3).

2.3. Laboratory analog synthesis

To synthesize POM under representative conditions of giant molecular clouds or presolar nebula, an experimental setup named OREGOC (French acronym for origin and evolution of ices and cometary organic compounds) (Fig. 2) similar to those described in Allamandola et al. (1988), Gerakines et al. (1995), Hagen et al. (1979) and Hudson and Moore (1995) is used. A Csl or a MgF₂ window is cooled down at about 20 K thanks to a closed-cycle helium cryostat (Advanced Research Systems, Inc.). Its temperature, measured by two thermocouples (type E and Au–Fe–Cr), is adjustable by means of a resistive heater driven with a temperature controller (Lakeshore). This window is located inside a high vacuum stainless steel chamber evacuated by a turbo pump (Varian turbo-V 301) backed up by a primary pump (Varian SH110). The pressure at room temperature is about 1×10^{-8} mbar. The ice evolution is monitored by FTIR.

POM is synthesized by the polymerization of formaldehyde catalyzed by ammonia (Schutte et al., 1993a). Ammonia (Air liquid, 99.995%) and formaldehyde² are deposited as ices on the cooled window through two independent tubes in order to prevent early reaction at ambient temperature. Once the H₂CO:NH₃ ices mixture is deposited at 20 K (Fig. 3), it is heated at 2 K/min. POM is produced during ice warming-up as already shown by Schutte et al. (1993a). At 293 K, the remaining sample is made only of POM (Fig. 4).

The synthesized POM is removed from the cryostat for further TOF-SIMS analysis, or kept inside the cryostat and heated at various temperatures (Table 1) in order to measure its lifetime as a function of temperature.

If only H₂CO ice is deposited on the window, no POM can be observed during the subsequent heating. The synthesis of POM requires a catalyst such as NH₃ (Schutte et al., 1993b). A H₂CO:NH₃ ratio close to 0.5 is used, as in this case the conversion of the initial H₂CO to POM is efficient (Schutte et al., 1993b).

The initial molecular ratio is derived from the IR spectra by integrating vibrational bands to estimate the column density of H₂CO and NH₃ according to their band strengths provided by the literature. For NH₃, the band strengths of the “umbrella” mode at 1070 cm⁻¹ is 1.7×10^{-17} cm/molecule (D’Hendecourt and Allamandola, 1986) and for H₂CO, the band strength at 2820 cm⁻¹ is 3.7×10^{-18} cm/molecule (Schutte et al., 1993b). We have tried to

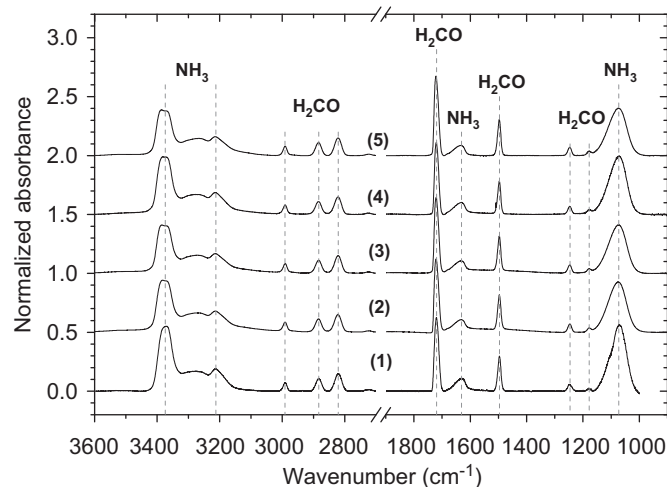


Fig. 3. FTIR spectra of ice deposit at 20 K for the five experiments presented in Table 1. All absorbances have been normalized to 0.15 at 2822 cm⁻¹ to compare the H₂CO:NH₃ ratio.

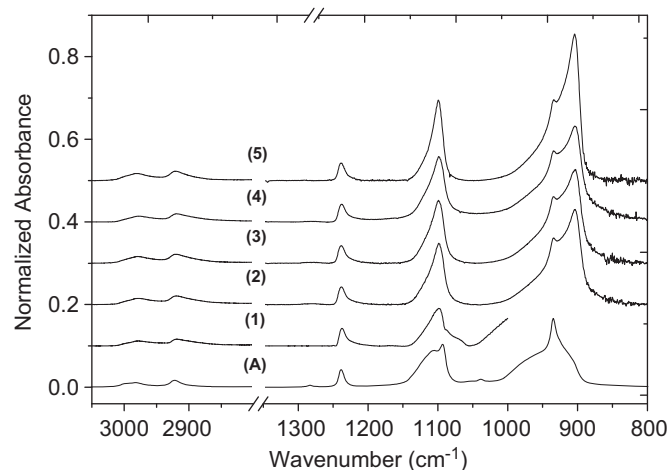


Fig. 4. FTIR spectra of POM at 293 K for the “POM Com” (A) and the five experiments (1–5) presented in Table 1. All absorbances have been normalized to 0.043 at 1238 cm⁻¹. Experiment no 1 has been performed on a MgF₂ substrate, which absorbs the IR beam below 1000 cm⁻¹.

reproduce similar gas ratio deposition for each experiment to obtain similar POM (see Table 1).

2.3.1. POM characterization by FTIR spectroscopy

Fig. 4 shows infrared spectra of the “POM Com” (A) and of the “POM Lab” samples (1–5). Table 2 lists the position of the infrared solid bands of the two kinds of POM as well as their attributions by Tadokoro et al. (1963) and Schutte et al. (1993b).

Some differences can be noticed between “POM Com” and “POM Lab” (Fig. 4). For instance, the major feature is located at 903 and 935 cm⁻¹ for “POM Lab” and “POM Com”, respectively. This difference may be interpreted by the solid state reorganization of “POM Com” structure induced by the pressure of the sample inside KBr pellets (Terlemezyan et al., 1978).

Four intense bands of POM, located at 903, 1099, 1238 and 2900 cm⁻¹, have been integrated. Between 3025 and 2850 cm⁻¹, IR spectra of POM display two features which are very close. So the integrated area at 2900 cm⁻¹ corresponds to the integration of both IR bands. The ratios of these areas are given in Table 1 and enlighten that the different “POM Lab” samples that we have synthesized are quite similar.

² Formaldehyde is produced by the thermal decomposition of commercial POM (Prolabo, >99.5%) because commercial formaldehyde is never sold as desired (i.e., with a purity >99%) and it always contains water or water and methanol. POM thermal degradation allows us to produce pure gaseous formaldehyde.

Table 1

Parameters of the experiments, H₂CO:NH₃ ratio for the ice mixture and also some properties of the synthesized POM.

N°	Comment		Ice mixture H ₂ CO:NH ₃	POM features: IR band ratio		
	POM nature	Experiment		903/ 1238	1099/ 1238	2900/ 1238
A	Commercial POM	TOF SIMS analysis	NA	16.7	7.4	1.8
1	POM Lab	TOF SIMS analysis	0.35	NA	8.2	2.6
2	POM Lab	Decomposition T=320 K	0.55	17.7	6.9	2.4
3	POM Lab	Decomposition T=330 K	0.57	18.1	6.9	2.5
4	POM Lab	Decomposition T=340 K	0.50	17.2	6.7	2.5
5	POM Lab	Decomposition T=350 K	0.63	24.8	7.9	2.7

Table 2

Assignments of POM FTIR features (Schutte et al., 1993b; Tadokoro et al., 1963); s, m and w correspond to strong, medium and weak intensity, respectively.

Vibrational mode	POM Com ν (cm ⁻¹)	POM Lab ν (cm ⁻¹)	Intensity
CH ₂ (rock.)–COC (sym. stretch.)		903	s
COC (sym. stretch.)+CH ₂ (rock.)	935	935	s
Unassigned	980		w
Unassigned	1038		s
COC (antisym. stretch.)–OCO (bend.)	1093		s
COC (sym. stretch.)+CH ₂ (rock.)		1099	s
Unassigned	1106		s
CH ₂ (rock.)+COC (bend.)–COC (sym. stretch.)	1238	1238	w
CH ₂ (twist)	1283	1283	w
CH ₂ /CH ₃ deformation	1382	1382	w
CH ₂ /CH ₃ deformation	1433	1433	w
CH ₂ /CH ₃ deformation	1469	1469	w
CH stretch.	2789	2790	m
CH stretch.	2922	2920	m
CH ₂ (antisym. stretch.)	2982	2979	m
Unassigned	2998		m

3. Results and discussion

The following section presents reference TOF-SIMS spectra, and their interpretation, of the two kinds of POM and their lifetimes for the temperature that cometary grains could encounter inside COSIMA. These data allow us to determine the best strategy to identify POM in cometary grains from observations of the COSIMA instrument.

3.1. POM characterization by a ground analog of COSIMA

3.1.1. Positive mode of the instrument

Fig. 5 displays the positive spectra of the “POM Com” and of a “POM Lab” sample from 1 to 300 Da, whereas both POMs show features from 1 to 600 Da. From each peak position, we have attributed the most likely molecular formula. Nevertheless it must be noted that with the resolving power of the instrument, each peak could be matched to several molecular formulae. Indeed the higher the mass is, the more molecular formulae possibility increases. In the present case, as the nature of the sample is known before measuring its mass spectrum, the molecular formula attribution is easier and relatively reliable. However due to the limited number of

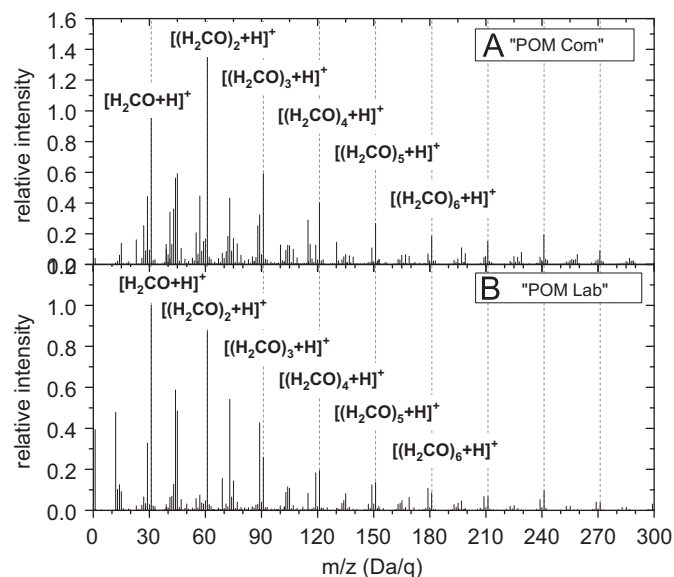


Fig. 5. Positive SIMS spectra of “POM Com” (A) and “POM Lab” (B). The figures present the relative intensities versus mass to charge ratio (m/z , in Da/q). Mass spectra are normalized to the intensity of peaks close to $m/z=30$.

secondary ions and the broad shape of the peaks beyond 300 Da, the molecular formula attributions with exact mass measured are very difficult. Nevertheless we assume that all these peaks belong to Polyoxymethylene.

Most intense peaks of both spectra are related to the monomer $[(H_2CO)+H]^+$ and its oligomers at mass $[(H_2CO)_n+H]^+$. Peaks related to oligomers fragmentation are also detected such as $[(H_2CO)_n-H]^+$, $[(H_2CO)_n+H-H_2O]^+$, $[(H_2CO)_n+H-OH]^+$, $[(H_2CO)_n+H-O]^+$, $[(H_2CO)_n+H-CH_2]^+$ and $[(H_2CO)_n+H-C]^+$ (Table 3). The different families of peaks are presented in Table 3. The peaks belonging to a family are separated by a mass of 30.011 Da, which is characteristic of POM positive spectra.

Both POMs share common features but the relative intensities of similar peaks are different. For instance, the intensities of peaks related to $[(H_2CO)_n-H]^+$ are higher for “POM Lab” than for the “POM Com”. This could be due to different chemical structure of the two POMs. POM Lab structure might facilitate the production of $[(H_2CO)_n-H]^+$ under the primary ion beam.

3.1.2. Negative mode of the instrument

Fig. 6 shows negative spectra of “POM Com” (A) and of “POM Lab” (B). Both spectra are quite similar. Their major peaks are those of hydrogen, oxygen and of hydroxyl ions. They also display features related to C⁻, CH⁻ and HCO₂⁻ at $m/z=44.999$. In the “POM Lab” spectrum (B), a peak related to Fluor anion can be observed. It comes from the MgF₂ substrate on which “POM Lab” has been synthesized. In “POM Com” spectrum (A), some peaks of cyanide and chloride (CN⁻ and Cl⁻) are also present. They are linked to the contamination of the target.

Apart for F⁻, CN⁻ and Cl⁻, all peaks detected could be characteristic of any oxygenated compounds. They cannot allow an unambiguous identification of POM. So, by itself, a negative spectrum of POM is not sufficient to identify clearly the presence of this compound.

However, it must be highlighted that negative spectra of POM provided by the Static SIMS Library 4 (2006), have a quite different appearance: the major peak is HCO₂⁻ anion at $m/z=44.999$ and it displays features with an alternating sequence of mass from 45 to 435 Da.

Table 3
List of the major spectral features identified thanks to their measured mass and classified in families. Only peaks between 1 and 300 Da are taken into account in this table because beyond 300 Da molecular formula attributions are very difficult due to the limited number of secondary ions and also to the broad shape of these peaks. The number of members corresponds to the number of molecules that the family contains. This table is adapted from the one presented in Bonnet et al. (submitted) for HCN polymers.

Family	POM Com			POM Lab		
	Number of members	<i>n</i> range for clearly identified molecules	<i>n</i> for most intense molecules	Number of members	<i>n</i> range for clearly identified molecules	<i>n</i> for most intense molecules
$[(\text{H}_2\text{CO})_n + \text{H}]^+$	10	1 to 10	2	10	1 to 10	1
$[(\text{H}_2\text{CO})_n - \text{H}]^+$	10	1 to 10	1	10	1 to 10	3
$[(\text{H}_2\text{CO})_n + \text{H} - \text{C}]^+$	10	1 to 10	1	8	1 to 9	1
$[(\text{H}_2\text{CO})_n + \text{H} - \text{CH}_2]^+$	10	1 to 10	1	10	1 to 10	1
$[(\text{H}_2\text{CO})_n + \text{H} - \text{O}]^+$	10	1 to 10	1	10	1 to 10	1
$[(\text{H}_2\text{CO})_n + \text{H} - \text{OH}]^+$	10	1 to 10	1	10	1 to 10	1
$[(\text{H}_2\text{CO})_n + \text{H} - \text{H}_2\text{O}]^+$	10	1 to 10	1	10	1 to 10	1

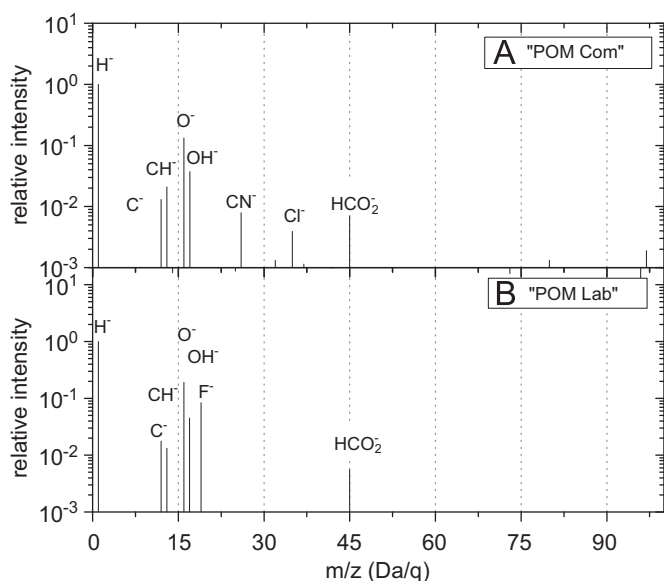


Fig. 6. Negative SIMS spectra of "POM Com" (A) and "POM Lab" (B). The figures show the relative intensity (in logarithm scale) versus mass to charge ratio (m/z). They have been normalized to the intensity of the peak at $m/z=1.008$.

In fact these differences between our spectra and the one from the Static SIMS library are hardly surprising as a different primary ion beam has been used for the two experiments. Our analysis is made with an Indium ion gun whereas the spectrum from the static SIMS library has been performed with a Cesium ion gun, which enhances the production of negative secondary ions from the sample (Hill, 2001). The sample preparation was also different: Polyoxymethylene has been washed in *n*-hexane and methanol before being mounted under a grid (no feature of *n*-hexane and methanol are observed in these spectra).

3.2. Detection of POM with COSIMA

The grains of 67P/CG are expected to be a complex mixture of minerals and organic compounds. Therefore the detection of POM in COSIMA spectra will not be easy even if as a pure compound it presents distinctive features.

In order to enhance the ability to detect POM presence in COSIMA spectra, mathematical methods for handling spectra could be useful. As observed, positive spectrum of POM displays a sequence of peaks with an alternation of mass 30.011. We now

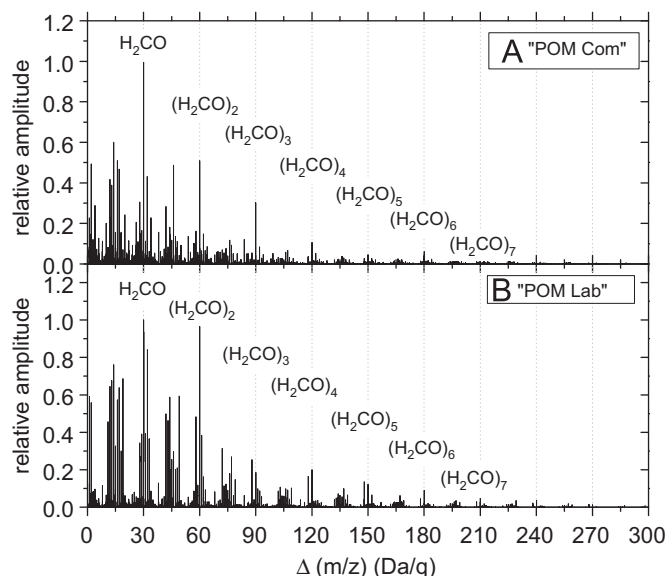


Fig. 7. Sum of peak intensity product as a function of the centroid difference $\Delta(m/z)$ with class interval width of 0.005 Da/q for commercial POM (A) and POM Lab (B). (A) ("POM Com") is normalized to the intensity at $\Delta(m/z)=30.013$. (B) ("POM Lab") is normalized to the intensity at $\Delta(m/z)=30.008$.

present a strategy to highlight this specific characteristic of the POM positive spectrum.

From the original mass spectrum, a peak detection algorithm is used to determine the centroid (m/z)_{*i*} and the intensity (I_i) of each peak having intensity higher than 100 counts. After this step, centroid differences $\Delta(m/z)$ between each pair of peaks in the spectrum are calculated as well as the product of the intensities of both considered peaks. The histogram showing the sum of peak intensity product as a function of the centroid difference $\Delta(m/z)$ with class interval width of 0.005 Da/q can be plotted. This procedure allows strengthening mass difference of the intense peaks present in the original mass spectrum. The histogram is shown in Fig. 7.

Those histograms present peaks up to 270 Da and most of them are, as for the spectra, separated from 30.011 Da. For both histograms, the most intense peak is located close to 30 Da. Some differences between these two histograms can be highlighted. For instance, the intensity of the peak at $\Delta(m/z)=60$ is higher in the "POM Lab" histogram than in the "POM Com" one (Fig. 7).

The major insight that brings the data treatment is that the peak widths in histograms are smaller than the corresponding peak widths in mass spectra. The decrease of the peak width is

illustrated in Fig. 8 for the peaks at 30 and 31 Da in histograms and in original mass spectra, respectively.

The peak close to 31 Da in the “POM Lab” mass spectrum is characterized by a centroid at $m/z=31.017$ and a FWHM of 0.030 whereas the peak close to 30 in the “POM Lab” histogram is characterized by a centroid at $\Delta(m/z)=30.012$ and a FWHM of 0.016. This treatment improves artificially the mass resolution by a factor 2 for “POM Lab” and by a factor of 4.4 for “POM Com”. Therefore it allows easier molecular formula attributions. For instance, the peak related to the monomer of POM in the mass spectrum ($m/z=31.017$) could be linked to 7 ions (CH_3O^+ : pseudo-molecular ion of POM monomer, SiH_3^+ , CH_5N^+ ...) considering the mass resolution, whereas the one from the data treatment could be associated only to 2 molecules (POM or aluminum hydride polymer).

The polymer of aluminum hydride $(\text{AlH}_3)_n$, named alane, is used as reducing agent in organic chemistry. Its monomer structure ($m/z=30.005$ Da) could interfere with formaldehyde at the instrumental resolution. Nevertheless this compound is currently only found under two forms: the monomer and the dimer structure. But Kawamura et al. (2003) show that $(\text{AlH}_3)_n$ with n up to 4 can form stable cyclic or polymeric structures. Therefore with only 3 oligomers, there is little chance to find a sequence of peaks alternating from 30.005 up to 270 Da provided by $(\text{AlH}_3)_n$.

So POM is the best candidate to explain these specific peaks alternation. These characteristic features on histograms could be easily interpreted by the loss of the same fragments (H, C, CH_2 , O, OH, H_2O and H_2CO) for all POM oligomers under the primary ion bombardment. The difference noticed at $\Delta(m/z)=60$ for the two histograms could be due to the preferential dimer loss during the fragmentation of the “POM Lab”. For “POM Lab”, an alternating sequence of peaks at $\Delta(m/z)$ equals $[(\text{H}_2\text{CO})_{n-2}\text{H}]$ is also observed. It could be due to the high intensity of peaks at mass $[(\text{H}_2\text{CO})_{n-1}\text{H}]^+$ in the “POM Lab” mass spectrum.

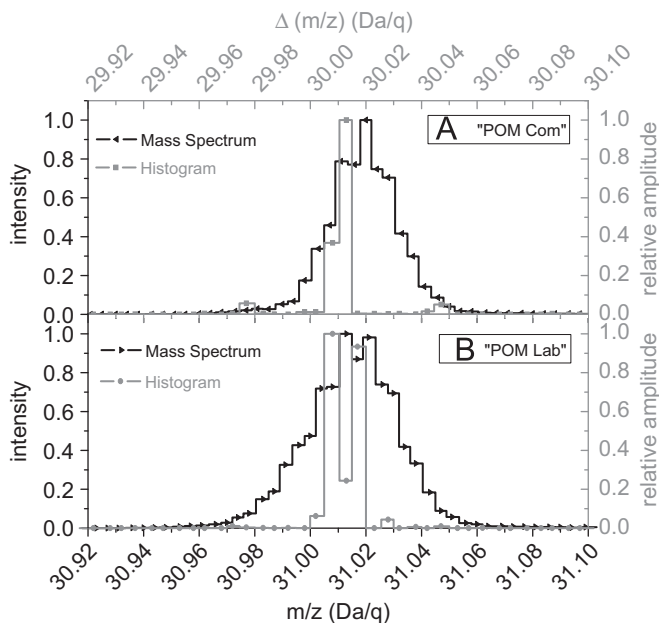


Fig. 8. Superposition of data treatment results (gray) and mass spectra (black) for “POM Com” (A) and “POM Lab” (B). The figures are focused on the peak linked to formaldehyde. Mass spectrum figures show the relative intensity versus mass to charge ratio (m/z). Mass spectra are normalized to the intensity at $m/z=30.020$ for “POM Com” and at $m/z=30.013$ for “POM Lab”. Histograms show the sum of peak intensity product as a function of the centroid difference $\Delta(m/z)$ with class interval width of 0.005 Da/q. Histograms are normalized to the intensity at $\Delta(m/z)=30.013$ for “POM Com” and at $\Delta(m/z)=30.008$ for “POM Lab”. The figure shows that the data treatment reduces the FWHM of peaks.

We have tested our method just with a spectrum of pure polyoxymethylene and it seems to allow its identification. But to really check its validity for COSIMA, it shall be tested on spectra of complex mixture containing POM. This point is however beyond the scope of this paper.

3.3. POM lifetime parameterization

POM in the solid phase can undergo a thermal decomposition into gaseous H_2CO at temperatures as low as 255 K (Grassie and Roche, 1968; Zimmermann and Behnisch, 1982; Fray et al., 2004). Between the cometary grain collection and their analysis, grains will be stored at a temperature close to 303 K (Kissel et al., 2007). Thus, if present in cometary grains, POM could undergo decomposition inside the COSIMA instrument. The thermal decomposition kinetics of POM samples, synthesized by heating $\text{H}_2\text{CO}:\text{NH}_3$ ice mixtures, has been parameterized to constrain when cometary grains have to be analyzed after their collection to maximize the chances to detect POM.

After being synthesized, four “POM Lab” samples have been kept at constant temperature (320, 330, 340 and 350 K) and monitored by FTIR (see Table 1). For each experiment, infrared spectra have been acquired with a time resolution of about 100 s and for each spectra the area of four infrared bands (903, 1099, 1238 and 2900 cm^{-1}) have been calculated. The initial time of decomposition is the time at which the temperature of the sample becomes constant. The temporal evolution of these four band’s area is shown in Fig. 9.

In Fig. 9, the POM decay predicted from the data published by Fray et al. (2004) is plotted using a first order kinetic law. It can be concluded that our experimental data do not follow first order kinetics, as commercial POM would. Indeed the rate of “POM Lab” disappearance decreases with time. A similar behavior has already been observed on POM thermal decomposition by Grassie and Roche (1968).

As previously mentioned, POM is a general name for formaldehyde polymers. It has been shown by Grassie and Roche (1968) that the kinetic of the thermal decomposition of POM depends on the average molecular weight of POM. Our samples are not

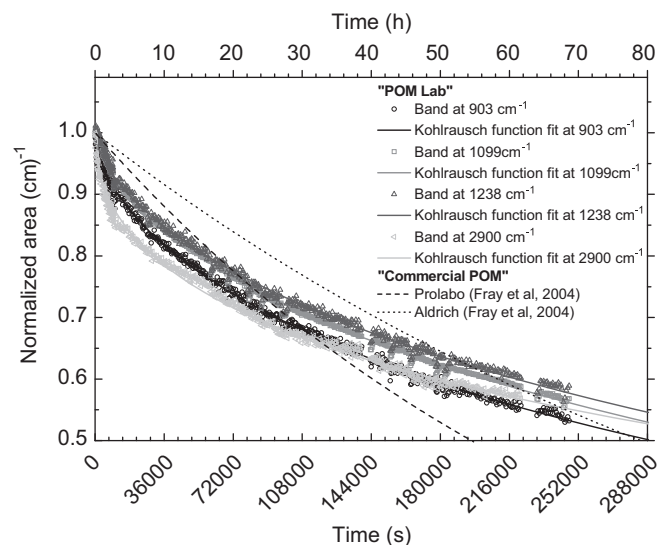


Fig. 9. Normalized area of four POM infrared bands as a function of time when submitted at 320 K. The bands at 903, 1099, 1238 and 2900 cm^{-1} are plotted in black, gray, dark gray and light gray, respectively. For each infrared band, a Kohlrausch relaxation function fit is shown. The temporal evolution predicted from Fray et al. (2004) on two different commercial POM provided by Prolabo (black dashed line) and Aldrich (black dotted line) is also plotted. These latter predictions have been calculated assuming a first order kinetic.

controlled in term of chain length and are most probably a mixture of polymers with various molecular weights.

For each POM molecule, if the thermal degradation follows first order kinetics, with a kinetic rate being a function of the chain length, the kinetic of decay of the whole POM sample should follow a Kohlrausch relaxation function (Plonka and Paszkiewicz, 1996). This function can be written:

$$N(t) = N_0 e^{-(kt)^\alpha} = N_0 e^{-(t/\tau_0)^\alpha} \quad (3)$$

$N(t)$ and N_0 being the number of molecules in the sample as a function of time and at initial time, respectively, α the dispersion parameter ranging from 0 to 1, k the mean kinetic rate (s^{-1}) and τ_0 the mean characteristic time (s) of decomposition.

The Kohlrausch relaxation function (Eq. (3)), related to dispersive kinetics, is fitted by “stretched” exponential curves (Plonka, 2001). These curves are characterized by two parts: at the beginning a sharp decrease and afterwards a much slower decline. This behavior could be explained either by chemical or physical processes such as not truly elementary reaction (i.e., species diffusion before reaction) or parallel reaction with different kinetics yielding to the same product, α reflecting the dispersion of the reaction rates compared to a mean value of k (Andraos, 2000; Plonka and Paszkiewicz, 1992, 1996; Siebrand and Wildman, 1986).

The time evolution of each studied band can be fitted with this model (Fig. 9). The parameters k and α , as well as their uncertainties, for each infrared band and for each experiment are reported in Table 4.

Grassie and Roche (1968) have shown that there is an inverse relationship between the thermal decomposition of POM kinetics and the average molecular weight of the sample. Therefore, the observed temporal evolution of POM could be due to the faster decomposition of the lighter polymers at the beginning of the experiment. It is then possible that the average molecular weight of the sample increases during the thermal degradation. Moreover, whereas it is very difficult to link the molecular weight of the polymer to its infrared spectrum, this interpretation could explain the fact that the time evolution of the infrared bands is different.

The mean kinetic constant (k , in s^{-1}) should follow the Arrhenius law (Eq. (4)). It is equal to the inverse of the characteristic time of degradation (τ_0 , in s)

$$k(T) = Ae^{-E_a/RT} \quad (4)$$

Table 4

Results of the fits with the Kohlrausch relaxation function (Eq. (3)) on the temporal evolution of each infrared band and for each experiment.

POM decomposition temperature (K)	IR band (cm^{-1})	k (s^{-1})	Δk (s^{-1})	A	$\Delta \alpha$	R^2
320	903	1.9E-06	2E-07	0.592	0.002	0.996
	1099	1.7E-06	1E-07	0.624	0.002	0.998
	1238	1.6E-06	2E-07	0.624	0.003	0.997
	2900	1.3E-06	1E-07	0.467	0.002	0.997
330	903	5.0E-06	6E-07	0.600	0.003	0.996
	1099	3.9E-06	3E-07	0.589	0.002	0.998
	1238	3.4E-06	3E-07	0.521	0.002	0.997
	2900	4.4E-06	4E-07	0.469	0.002	0.997
340	903	4.9E-05	1.2E-05	0.513	0.006	0.984
	1099	3.9E-05	7E-06	0.545	0.005	0.992
	1238	3.5E-05	6E-06	0.565	0.005	0.993
	2900	2.2E-05	8E-06	0.461	0.008	0.968
350	903	6.4E-05	1.1E-05	0.619	0.006	0.983
	1099	6.3E-05	5E-06	0.612	0.002	0.997
	1238	6.1E-05	9E-06	0.619	0.004	0.990
	2900	1.6E-05	6E-06	0.368	0.006	0.940

where A is the frequency factor (s^{-1}), E_a the activation energy ($J mol^{-1}$) and R the universal gas constant ($J mol^{-1} K^{-1}$) and T the temperature (K). Fig. 10 displays the natural logarithm of the mean kinetic constant as a function of the inverse of the temperature. These measurements are well fitted using an Arrhenius law (Fig. 10). This fit allows to estimate $E_a=113$ ($\pm 4\%$) $kJ mol^{-1}$ and $\ln A=29$ ($\pm 41\%$). Since the kinetic constants derived from the Kohlrausch relaxation function are actually average values, E_a and A values are relevant to the parameterization of the mean kinetic constant as a function of the temperature.

Knowing these values, the mean characteristic time of POM decomposition can be estimated for any temperature. Whatever the kinetic parameterization is, we can define the characteristic time of decomposition as the inverse of k (see Eq. (3)). It corresponds to the duration after which 37% of the initial sample of POM is remaining (diminution by a factor e).

COSIMA samples can encounter temperature between 253 and 303 K. Fig. 11 displays the mean characteristic time of POM decomposition as a function of the temperature calculated from

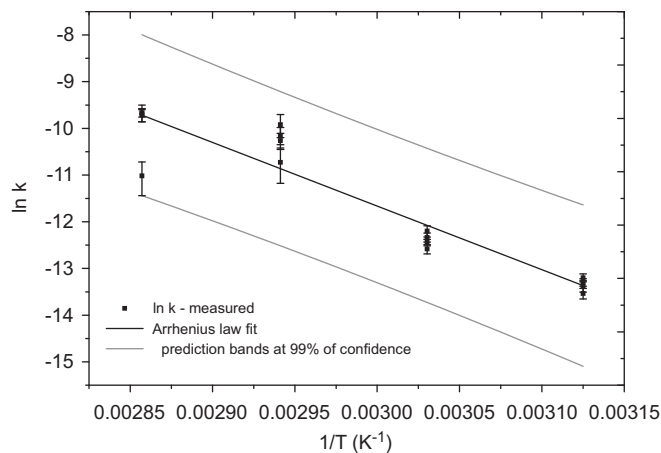


Fig. 10. Natural logarithm of the POM decomposition kinetic rate as a function of the inverse of the temperature. The black dots are experimental measurements and the black line is the best fit with a linear function allowing us to measure the activation energy (E_a) and the frequency factor (A) of the Arrhenius law. The gray lines are the predictions bands of Arrhenius law at a level of 99% of confidence.

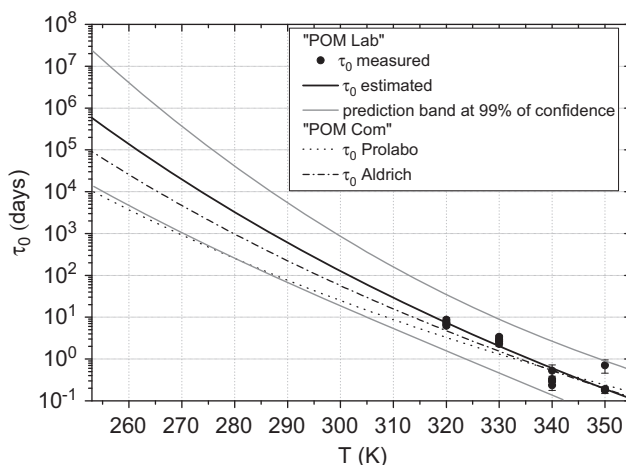


Fig. 11. Mean characteristic times of POM decomposition as a function of the temperature. The black dots are experimental measurements and the black curve is the extrapolation of our measurements using the Arrhenius law measured in this work. The gray curves are the predictions bands at a level of 99% of confidence. The dotted and dash-dotted curves are the characteristic times of POM decomposition calculated from Fray et al. (2004).

our measurements using a Kohlrausch relaxation function (see Eq. (3)) and from the measurements published by Fray et al. (2004) on two different commercial samples using a first order kinetics for the temperature range that cometary grains could encounter inside COSIMA.

The characteristic times calculated using the data of Fray et al. (2004) fall in the interval of 99% of confidence except below 280 K for the “Commercial POM” from Prolabo (Fig. 11). Our measurements are in quite good agreement with these previous data, even if the parameterization of the kinetics depends on the source of POMs, and although characteristic times of POM decomposition could differ by almost an order of magnitude when extrapolated at low temperature.

After grain collection, the COSIMA target can be stored before analysis. During this storage, the temperature of the target and then of the collected cometary grains can reach 303 K (Kissel et al., 2007). At this temperature, according to our parameterization, the mean characteristic time of POM decomposition is at least 15 days. Thus, if during the storage stage the cometary grains do not encounter temperature higher than 303 K, the POM, if present in cometary grains, will decompose slowly. In such case the storage of the target will not prevent the detection of POM. It must be kept in mind that the delay between new programming operations from Earth and their application in space is about 1 week. Thus, the decomposition of POM has to be taken into account to decide the space operation of COSIMA. In order to maximize the chance to detect POM in cometary grains, the analysis of the collected grains has to be done as quickly as possible.

To check the presence of POM on cometary grains, the chemistry station integrated in COSIMA could also be used. Indeed, in the chemistry station, the target and the collected grains can be heated up to 403 K. At this temperature, the mean lifetime of POM is lower than 17 min. Therefore if two analyses are made, one just after the sample collection, the second one after the sample heating, then confirmation of the presence of POM can be highlighted by the disappearance of specific POM features in the mass spectra.

4. Conclusion

COSIMA is a decisive instrument for the characterization of solid compounds ejected from the nucleus of comet 67P/CG and more especially of refractory organic molecules. If there is some POM in the grains of 67P/CG, it is feasible to detect it in the positive mode of the instrument, provided that its signature is not drowned by the other cometary organic compounds. Mathematical treatment of the data will be a useful tool to highlight the presence of POM in mass spectra of complex mixture. POM can be identified thanks to its specific alternation in mass (30.011 Da) of these peaks and also thanks to its specific fragmentation pattern. As POM is a thermally unstable compound, cometary grains have to be analyzed within a fortnight after their collection in order to maximize chances to observe the features of this polymer.

COSIMA has one of the best resolutions for a spaceborne mass spectrometer since the beginning of cometary space exploration. It will allow an easier identification of compounds compared to the mass spectrometers onboard Vega 1 & 2, Giotto and Stardust. However, current specifications of such instruments are far from resolving all the ambiguities in mass spectra of complex organic mixture. Only instruments with very high resolution capabilities, such as the one achieved with the commercial Orbitrap instrument in the laboratory, at about 100 000 (Hu et al., 2005), are fully adapted to in situ analysis of complex organic mixtures in the Solar System. Such instruments should be adapted to space

and considered as being part of the payload of future space missions.

Acknowledgment

This work has been supported by CNES (Centre National des Etudes Spatiales – French space agency) and region Centre, L.L.R. is the recipient of a CNES/Région Centre fellowship.

References

- Allamandola, L.J., Sandford, S.A., Valero, G.J., 1988. Photochemical and thermal evolution of interstellar/precometary ice analogs. *Icarus* 76, 225–252.
- Anders, E., 1989. Pre-biotic organic matter from comets and asteroids. *Nature* 342, 255–257.
- Andraos, J., 2000. Biomolecular kinetics at low temperature using FTIR matrix isolation spectroscopy: some caveats. Thermokinetic parameters for the reaction of fulveones with pyridine in pyridine matrixes. *Journal of Physical Chemistry* 104, 1532–1543.
- Bernstein, M.P., Sandford, S.A., Allamandola, L.J., Chang, S., Scharberg, M.A., 1995. Organic compounds produced by photolysis of realistic interstellar and cometary ice analogs containing methanol. *Asia Pacific Journal* 454, 327–344.
- Bevington, J.C., May, H., 1964. aldehyde polymers. *Encyclopedia of polymer science and technology*, 609–628.
- Bockelée-Morvan, D., Crovisier, J., Mumma, M.J., Weaver, H.A., Keller, H.U., Weaver, H.A., 2004. The composition of cometary volatiles. In: Festou, M.C., Keller, H.U., Weaver, H.A. (Eds.), *Comets II*. The University of Arizona Press, Tucson, USA, pp. 391–423.
- Bonnet, J.-Y., Thissen, R., Frisari, M., Vuitton, V., Quirico, E., Orthous-Daunay, F.-R., Dutuit, O., Le Roy, L., Fray, N., Cottin, H., Hörst, S.M., Yelle, R.V., submitted. Structure and composition of HCN polymer through high resolution mass spectrometry. *International Journal of Mass Spectrometry*.
- Brownlee, D., Tsou, P., Aleon, J., Alexander, C., Araki, T., Bajt, S., Baratta, G., Bastien, R., Bland, P., Bleuët, P., Borg, J., Bradley, J., Brearley, A., Brenker, F., Brennan, S., Bridges, J., Browning, N., Brucato, J., Bullock, E., Burchell, M., Busemann, H., Butterworth, A., Chaussidon, M., Chevront, A., Chi, M., Cintala, M., Clark, B., Clemett, S., Cody, G., Colangeli, L., Cooper, G., Cordier, P., Daghlian, C., Dai, Z., D'Hendecourt, L., Djouadi, Z., Dominguez, G., Duxbury, T., Dworkin, J., Ebel, D., Economou, T., Fakra, S., Faurey, S., Fallon, S., Ferrini, G., Ferroir, T., Fleckenstein, H., Floss, C., Flynn, G., Franchi, I., Fries, M., Gainsforth, Z., Gallien, J.-P., Genge, M., Gilles, M., Gillet, P., Gilmour, J., Glavin, D., Gounelle, M., Grady, M., Graham, G., Grant, P., Green, S., Grossemy, F., Grossman, L., Grossman, J., Guan, Y., Hagiya, K., Harvey, R., Heck, P., Herzog, G., Hoppe, P., Horz, F., Huth, J., Hutcheon, I., Ignatyev, K., Ishii, H., Ito, M., Jacob, D., Jacobsen, C., Jacobsen, S., Jones, S., Joswiak, D., Jurewicz, A., Kearsley, A., Keller, L., Khodja, H., Kilcoyne, A., Kissel, J., Krot, A., Langenhorst, F., Lanzirotti, A., Le, L., Leshin, L., Leitner, J., Lemelle, L., Leroux, H., Liu, M.-C., Luening, K., Lyon, I., MacPherson, G., Marcus, M., Marhas, K., Marty, B., Matrajt, G., McKeegan, K., Meibom, A., Mennella, V., Messenger, K., Messenger, S., Mikouchi, T., Mostefaoui, S., Nakamura, T., Nakano, T., Newville, M., Nittler, L., Ohnishi, I., Ohsumi, K., Okudaira, K., Papanastassiou, D., Palma, R., Palumbo, M., Pepin, R., Perkins, D., Perronnet, M., Pianetta, P., Rao, W., Rietmeijer, F., Robert, F., Rost, D., Rotundi, A., Ryan, R., Sandford, S., Schwandt, C., See, T., Schlutter, D., Sheffield-Parker, J., Simionovici, A., Simon, S., Sittinsky, I., Snead, C., Spencer, M., Stadermann, F., Steele, A., Stephan, T., Stroud, R., Susini, J., Sutton, S., Suzuki, Y., Taheri, M., Taylor, S., Teslich, N., Tomeoka, K., Tomioka, N., Toppani, A., Trigo-Rodriguez, J., Troadec, D., Tsuchiyama, A., Tuzzolino, A., Tyliczszak, T., Uesugi, K., Velbel, M., Vellenga, J., Vicenzi, E., Vincze, L., Warren, J., Weber, I., Weisberg, M., Westphal, A., Wirick, S., Wooden, D., Wopenka, B., Wozniakiewicz, P., Wright, I., Yabuta, H., Yano, H., Young, E., Zare, R., Zega, T., Ziegler, K., Zimmerman, L., Zinner, E., Zolensky, M., 2006. Comet 81P/Wild 2 under a microscope. *Science* 314, 1711–1716.
- Chyba, C., Sagan, C., 1992. Endogenous production, exogenous delivery and impact-shock synthesis of organic molecules: an inventory for the origins of life. *Nature* 355, 125–132.
- Coradini, A., Capaccioni, F., Drossart, P., Arnold, G., Ammannito, E., Angrilli, F., Barucci, A., Bellucci, G., Benkhoff, J., Bianchini, G., Bibring, J., Blecka, M., Bockelée-Morvan, D., Capria, M., Carlson, R., Carsenty, U., Cerroni, P., Colangeli, L., Combes, M., Combi, M., Crovisier, J., Desanctis, M., Encrenaz, E., Erard, S., Federico, C., Filacchione, G., Fink, U., Fonti, S., Formisano, V., Ip, W., Jaumann, R., Kuehrt, E., Langevin, Y., Magni, G., McCord, T., Mennella, V., Mottola, S., Neukum, G., Palumbo, P., Piccioni, G., Rauer, H., Saggini, B., Schmitt, B., Tiphene, D., Tozzi, G., 2007. Virtis: an imaging spectrometer for the Rosetta Mission. *Space Science Reviews* 128, 529–559.
- Cottin, H., Bénéilan, Y., Gazeau, M.-C., Raulin, F., 2004. Origin of cometary extended sources from degradation of refractory organics on grains: polyoxymethylene as formaldehyde parent molecule. *Icarus* 167, 397–416.
- Cottin, H., Fray, N., 2008. Distributed sources in comets. *Space Science Reviews* 138, 179–197.
- Crovisier, J., Leech, K., Bockelée-Morvan, D., Brooke, T.Y., Hanner, M.S., Altieri, B., Keller, H.U., Lellouch, E., 1997. The spectrum of comet Hale-Bopp (C/1995 O1)

- observed with the infrared space observatory at 2.9 astronomical units from the Sun. *Science* 275, 1904–1907.
- D'Hendecourt, L., Allamandola, L.J., 1986. Time dependant chemistry in dense molecular cloud. III. Infrared band cross section of molecules in the solid state in 10 K. *Astronomy and Astrophysics Supplement* 64, 453–467.
- Delsemme, A.H., 1999. The deuterium enrichment observed in recent comets is consistent with the cometary origin of seawater. *Physica Status Solidi* 47, 125–131.
- Elsila, J.E., Glavin, D.P., Dworkin, J.P., 2009. Cometary glycine detected in samples returned by Stardust. *Meteoritics & Planetary Science* 44, 1323–1330.
- Feldman, P.D., Cochran, A.L., Combi, M.R., 2004. Spectroscopic investigation of fragment species in the coma. In: Festou, M.C., Keller, H.U., Weaver, H.A. (Eds.), *Comets II*. The University of Arizona Press, Tucson, USA, pp. 425–447.
- Fomenkova, M., Chang, S., Mukhin, L.M., 1994. Carbonaceous components in the comet Halley dust. *Geochimica et Cosmochimica Acta* 58, 4503–4512.
- Fray, N., Bénilan, Y., Biver, N., Bockelée-Morvan, D., Cottin, H., Crovisier, J., Gazeau, M.-C., 2006. Heliocentric evolution of the degradation of polyoxymethylene: application to the origin of the formaldehyde (H₂CO) extended source in comet C/1995 O1 (Hale-Bopp). *Icarus* 184, 239–254.
- Gerakines, P.A., Schutte, W.A., Greenberg, J.M., Van Dishoeck, E.F., 1995. The infrared band strengths of H₂O, CO and CO₂ in laboratory simulations of astrophysical ice mixture. *Astronomy & Astrophysics* 296, 810–818.
- Glassmeier, K.-H., Boehnhardt, H., Koschny, D., Kürt, E., Richter, I., 2007. The Rosetta mission: flying towards the origin of the solar system. *Space Science Reviews* 128, 1–21.
- Goesmann, F., Rosenbauer, H., Roll, R., Szopa, C., Raulin, F., Sternberg, R., Israel, G., Meierhenrich, U., Thiemann, W., Muñoz-Caro, G., 2007. COSAC, the cometary sampling and composition experiment on philae. *Space Science Reviews* 128, 257–280.
- Hagen, W., Allamandola, L.J., Greenberg, J.M., 1979. Interstellar molecule formation in grains mantles: the laboratory analog experiments, results and implication. *Astrophysics and Space Science* 65, 215–240.
- Hill, R., 2001. Primary ion beam systems. In: Vickerman, J.C., Briggs, D. (Eds.), *TOF-SIMS. surface analysis by mass spectrometry*. IM Publications & SurfaceSpectra Limited, pp. 95–113.
- Hu, Q., Noll, R.J., Li, H., Makarov, A., Hardman, M., Graham Cooks, R., 2005. The orbitrap: a new mass spectrometer. *Journal of Mass Spectrometry* 40, 430–443.
- Hudson, R.L., Moore, M.H., 1995. Far-IR spectral changes accompanying proton irradiation of solids of astrochemical interest. *Radiation Physics and Chemistry* 45, 779–789.
- Huebner, W.F., 1987. First polymer in space identified in comet Halley. *Science* 237, 628–630.
- Irvine, W.M., Lunine, J.I., 2004. The cycle of matter in our galaxy: from clouds to comets. In: Festou, M.C., Keller, H.U., Weaver, H.A. (Eds.), *Comets II*. University of Arizona Press, Tucson, USA, pp. 25–31.
- Jessberger, E.K., Cristoforidis, A., Kissel, J., 1988. Aspects of the major element composition of Halley's dust. *Nature* 332, 691–695.
- Kawamura, H., Kumar, V., Sun, Q., Kawazoe, Y., 2003. Cyclic and linear polymeric structures of Al_nH_{3n} (n=3–7) molecules. *Physical Review A* 67, 063205. id.
- Kissel, J., Altwegg, K., Clark, B.C., Colangeli, L., Cottin, H., Czernopiel, S., Eibl, J., Engrand, C., Fehring, H.M., Feuerbacher, B., Fomenkova, M., Glasmachers, A., Greenberg, J.M., Grün, E., Haerendel, G., Henkel, H., Hilchenbach, M., von Hoerner, H., Höfner, H., Hornung, K., Jessberger, E.K., Koch, A., Krüger, H., Langevin, Y., Parigger, P., Raulin, F., Rüdener, F., Rynö, J., Schmid, E.R., Schulz, R., Silén, J., Steiger, W., Stephan, T., Thirkell, L., Thomas, R., Torkar, K., Utterback, N.G., Varmuza, K., Wanczek, K.P., Werther, W., Zschege, H., 2007. Cosima: high resolution time-of-flight secondary ion mass spectrometer for the analysis of cometary dust particles onboard Rosetta. *Space Science Reviews* 128, 823–867.
- Kissel, J., Brownlee, D.E., Buchler, K., Clark, B.C., Fechtig, H., Grün, E., Hornung, K., Igenbergs, E.B., Jessberger, E.K., Krueger, F.R., Kuczer, H., McDonnell, J.A.M., Morfill, G.M., Rahe, J., Schwehm, G.H., Sekanina, Z., Utterback, N.G., Volk, H.J., Zook, H.A., 1986a. Composition of comet Halley dust particles from Giotto observations. *Nature* 321, 336–337.
- Kissel, J., Krueger, F.R., Silen, J., Clark, B.C., 2004. The cometary and interstellar dust analyser at comet 81P/Wild2. *Science* 304, 1774–1776.
- Kissel, J., Sagdeev, R.Z., Bertaux, J.L., Angarov, V.N., Audouze, J., Blamont, J.E., Buchler, K., Evlanov, E.N., Fechtig, H., Fomenkova, M.N., von Hoerner, H., Inogamov, N.A., Khromov, V.N., Knabe, W., Krueger, F.R., Langevin, Y., Leonasv, B., Levasseur-Regourd, A.C., Managadze, G.G., Podkolzin, S.N., Shapiro, V.D., Tabaldyev, S.R., Zubkov, B.V., 1986b. Composition of comet Halley dust particles from VEGA observations. *Nature* 321, 280–282.
- Krueger, F.R., Kissel, J., 1987. The chemical composition of the dust of comet P/Halley as measured by PUMA on board VEGA-1. *Naturwissenschaften* 74, 312–316.
- Langevin, Y., Kissel, J., Bertaux, J.L., Chassefière, E., 1987. First statistical analysis of 5000 mass spectra of cometary grains obtain by PUMA 1 (Vega 1) and PIA (Giotto) impact ionization mass spectrometers in the compressed modes. *Astronomy and Astrophysics* 187, 761–766.
- Lawler, M.E., Brownlee, D.E., Temple, S., Wheelock, M.M., 1989. Iron, magnesium, and silicon in dust from comet Halley. *Icarus* 80, 225–242.
- Mitchell, D.L., Lin, R.P., Carlson, C.W., Korth, A., Rème, H., Mendis, D.A., 1992. The origin of complex organic ions in the coma of comet Halley. *Icarus* 98, 125–133.
- Oro, J., 1961. Comets and formation of biochemical compounds on the primitive Earth. *Nature* 190, 389–390.
- Oro, J., Lazzano, A., Ehrenfreund, P., 2006. In: Thomas, P.J., Hicks, R.D., Chyba, C.F., Mckay, C.P. (Eds.), *Comets and the Origin and Evolution of Life*, 2nd edn. Springer, pp. 1–18.
- Pchelintsev, V.V., Sokolov, A.Y., Zaikov, G.E., 1988. Kinetic principles and mechanisms of hydrolytic degradation of mono- and polyacetals – A review. *Polymer Degradation and Stability* 21, 285–310.
- Plonka, A., 2001. Dispersive kinetics. *Annual Reports on the Progress of Chemistry, Section C: Physical Chemistry* 97, 91–147.
- Plonka, A., Paszkiewicz, A., 1992. Kinetics in dynamically disorder systems: time scale dependence of reaction patterns in condensed media. *Journal of Chemical Physics* 96, 1128–1133.
- Plonka, A., Paszkiewicz, A., 1996. Phenomenological interpretation of kinetics with time dependent specific reaction rates. *Chemical Physics* 212, 1–8.
- Sandford, S.A., Aleon, J., Alexander, C.M.O.D., Araki, T., Bajt, S., Baratta, G.A., Borg, J., Bradley, J.P., Brownlee, D.E., Brucato, J.R., Burchell, M.J., Busemann, H., Butterworth, A., Clemett, S.J., Cody, G., Colangeli, L., Cooper, G., D'Hendecourt, L., Djouadi, Z., Dworkin, J.P., Ferrini, G., Fleckenstein, H., Flynn, G.J., Franchi, I.A., Fries, M., Gillet, M.K., Glavin, D.P., Gounelle, M., Grosse, F., Jacobsen, C., Keller, L.P., Kilcoyne, A.L.D., Leitner, J., Matrajt, G., Meibom, A., Mennella, V., Mostefaoui, S., Nittler, L.R., Palumbo, M.E., Papanastassiou, D.A., Robert, F., Rotundi, A., Snead, C.J., Spencer, M.K., Stadermann, F.J., Steele, A., Stephan, T., Tsou, P., Tyliszczak, T., Westphal, A.J., Wirick, S., Wopenka, B., Yabuta, H., Zare, R.N., Zolensky, M.E., 2006. Organics captured from comet 81P/Wild 2 by the Stardust Spacecraft. *Science* 314, 1720–1724.
- Sandford, S.A., Bajt, S., Clemett, S.J., Cody, G.D., Cooper, G., Degregorio, B.T., de Vera, V., Dworkin, J.P., Elsila, J.E., Flynn, G.J., Glavin, D.P., Lanzirrotti, A., Limerio, T., Martin, M.P., Snead, C.J., Spencer, M.K., Stephan, T., Westphal, A., Wirick, S., Zare, R.N., Zolensky, M.E., 2010. Assessment and control of organic and other contaminants associated with the Stardust sample return from comet 81P/Wild 2. *Meteoritics & Planetary Science* 45, 406–433.
- Schutte, W., Allamandola, L., Sandford, S., 1993a. Formaldehyde and organic molecule production in astrophysical ices at cryogenic temperatures. *Science* 259, 1143–1145.
- Schutte, W.A., Allamandola, L.J., Sandford, S.A., 1993b. An experimental study of the organic molecules produced in cometary and interstellar ice analogs by thermal formaldehyde reactions. *Icarus* 104, 118–137.
- Siebrand, W., Wildman, T.A., 1986. Dispersive kinetics: a structural approach to nonexponential processes in disordered media. *Accounts of Chemical Research* 19, 238–243.
- Tadokoro, H., Kobayashi, M., Kawaguchi, Y., Kobayashi, A., Murahashi, S., 1963. Normal vibration of the polymer molecules of helical configuration. III. Polyoxymethylene and polyoxymethylene-d₂. *Journal of Chemical Physics* 38, 703–721.
- Terlemezyan, L., Mihailov, M., Schmidt, P., Schneider, B., 1978. Conformational changes of poly(oxyethylene) induced by pressure and mechanical treatment. *Makromolekulare Chemie* 179, 807–813.
- The Static SIMS Library, 2006. In: Vickerman, J.C., Briggs, D., Henderson, A. (Eds.), *SurfaceSpectra*, 4. Manchester, UK.
- Vinogradoff, V., Duvernay, F., Danger, G., Theulé, P., Chivassa, T., 2011. New insight into the formation of hexamethylenetetramine (HMT) in interstellar and cometary ice analogs. *Astronomy and Astrophysics* 530. id.A128.
- Walker, J., 1964. *Formaldehyde*, 3rd edn. Reinhold, New York.
- Wright, I.P., Barber, S.J., Morgan, G.H., Morse, A.D., Sheridan, S., Andrews, D.J., Maynard, J., Yau, D., Evans, S.T., Leese, M.R., Zarnecki, J.C., Kent, B.J., Waltham, N.R., Whalley, M.S., Heys, S., Drummond, D.L., Edson, R.L., Sawyer, E.C., Turner, R.F., Pillinger, C.T., 2007. Ptolemy an instrument to measure stable isotopic ratios of key volatiles on a cometary nucleus. *Space Science Reviews* 128, 363–381.
- Zimmermann, H., Behnisch, J., 1982. Thermogravimetric investigations on the kinetics of thermal degradation of polyoxymethylenes. *Thermochimica Acta* 59, 1–8.
- Zolensky, M.E., Zega, T.J., Yano, H., Wirick, S., Westphal, A.J., Weisberg, M.K., Weber, I., Warren, J.L., Velbel, M.A., Tsuchiyama, A., Tsou, P., Toppani, A., Tomioka, N., Tomeoka, K., Teslich, N., Taheri, M., Susini, J., Stroud, R., Stephan, T., Stadermann, F.J., Snead, C.J., Simon, S.B., Simionovici, A., See, T.H., Robert, F., Rietmeijer, F.J.M., Rao, W., Perronnet, M.C., Papanastassiou, D.A., Okudaira, K., Ohsumi, K., Ohnishi, I., Nakamura-Messenger, K., Nakamura, T., Mostefaoui, S., Mikouchi, T., Meibom, A., Matrajt, G., Marcus, M.A., Leroux, H., Lemelle, L., Le, L., Lanzirrotti, A., Langenhorst, F., Krot, A.N., Keller, L.P., Kearsley, A.T., Joswiak, D., Jacob, D., Ishii, H., Harvey, R., Hagiya, K., Grossman, L., Grossman, J.N., Graham, G.A., Gounelle, M., Gillet, P., Genge, M.J., Flynn, G., Ferroir, T., Fallon, S., Ebel, D.S., Dai, Z.R., Cordier, P., Clark, B., Chi, M., Butterworth, A.L., Brownlee, D.E., Bridges, J.C., Brennan, S., Brearley, A., Bradley, J.P., Bleuett, P., Bland, P.A., Bastien, R., 2006. Mineralogy and petrology of comet 81P/Wild 2 nucleus samples. *Science* 314, 1735–1739.